Short communication

Structural and electrical properties of BaCe(Ti,Y)O$_3$ protonic conductors

P. Pasierb*, M. Osiadły, S. Komornicki, M. Rekas

AGH University of Science and Technology, Faculty of Materials Science and Ceramics, al. Mickiewicza 30, 30-059 Krakow, Poland

ABSTRACT

Barium cerate exhibits high protonic conductivity, especially when doped by suitable trivalent ions. A possible approach to get the protonic conductor stable in the presence of CO_2 with relatively high protonic conductivity is the preparation of solid solutions of $BaCe_{1-x}Me_xO_{3-\delta}$ (Me = Zr, Ti) doped simultaneously with acceptor ion. In this work selected properties of series of $Ba(Ce_{0.95}Ti_{0.05})_{1-y}Y_yO_{3-\delta}$ ($0 \leq y \leq 0.2$) materials prepared by solid-state reaction method were investigated. X-ray diffraction (XRD), scanning electron microscopy (SEM) and direct current (DC) electrical measurements, including open cell voltage (OCV) measurements of electrochemical cells were used as experimental techniques. Structural studies have shown materials crystallized in orthorhombic Pmcn phase with the solubility limit of Y in $Ba(Ce_{0.95}Ti_{0.05})_{1-y}Y_yO_{3-\delta}$ higher than 20 at.%. The DC conductivity measurements accompanied by the potentiometric OCV measurements of solid state electrochemical cells in controlled gas atmospheres (containing H_2, O_2 and H_2O) and temperatures (500–800 °C) allowed determination of total electrical conductivity and transference numbers of oxygen, protonic and electronic defects in prepared materials. The introduction of Y increases total electrical conductivity and transference numbers for protonic defects, which was correlated with structural changes.

© 2011 Elsevier B.V. All rights reserved.

1. Introduction

Cerium-based perovskites are an attractive family of materials for some intermediate and high temperature applications. These materials exhibit relatively high proton conductivities at intermediate temperatures (in the range of 400–800 °C) after exposure to water or hydrogen containing atmospheres [1]. The construction of fuel cells or other electrochemical devices such as hydrogen pumps, sensors and specific reactors based on such ceramic proton conducting solid electrolytes will be economically possible when materials with high protonic conductivity and good chemical stability, especially in the presence of CO_2, are developed.

The creation of protonic defects takes place in the presence of water vapor (or hydrogen) according to the following reaction:

$$H_2O_{(g)} + V_O^{\bullet\bullet} + O_O^x \Leftrightarrow 2(OH)_O^{\bullet} \qquad (1)$$

High concentration of oxygen vacancies, necessary for formation of protonic defects leading to the material with protonic conductivity at required level may be obtained by acceptor doping according to the reaction (where M^{3+} denotes cation of dopant introduced into $BaCeO_3$ lattice):

$$M_2O_3 + 2BaO \Rightarrow 2Ba_{Ba} + 2M'_{Ce} + V_O^{\bullet\bullet} + 5O_O \qquad (2)$$
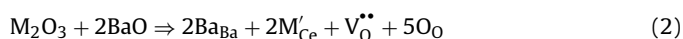
Several dopants such as Yb_2O_3 [2–4], Gd_2O_3 [5], Nd_2O_3 [6–8], Y_2O_3 [7,9,10] have been proposed in order to increase the protonic conductivity, with reasonable success.

Another problem to be solved is the poor chemical stability of some of these materials in real working conditions. Prolonged exposure to CO_2-containing atmospheres leads to the deterioration of mechanical properties of material, due to formation of secondary barium carbonate and cerium oxide [11,12]. The formation of solid solutions with chemically stable, isostructural $BaZrO_3$ is the successful approach to the improvement of corrosion resistance against the CO_2. Unfortunately, the introduction of Zr leads to the dramatic decrease of electrical conductivity of the material [13]. Our previous works [14–16] have shown that introduction of titanium into $BaCeO_3$ led to the improvement of chemical stability in the presence of CO_2. In parallel, the total electrical conductivity was decreased together with decrease of protonic and the increase of electronic transference numbers in studied materials. These results are similar to that observed for Zr-substituted $BaCeO_3$, as mentioned above. Presented literature search indicate that one of the ways to obtain materials with high protonic conductivity and good chemical stability is the proper selection of suitable chemical composition by doping cerate-based material with foreign ions. The simultaneous doping by Ti and Y seems to be the proper approach to the material with optimal chemical stability and high protonic and total electrical conductivity.

The purpose of this work was to investigate the influence of Ti and Y dopants on the structural and electrical properties of $BaCeO_3$

* Corresponding author. Tel.: +48 12 617 25 33; fax: +48 12 617 24 93.
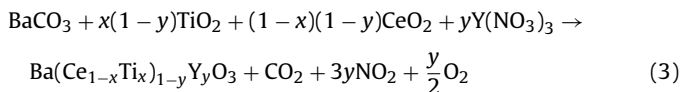 *E-mail address:* ppasierb@agh.edu.pl (P. Pasierb).

materials. $Ba(Ce_{1-x}Ti_x)_{1-y}Y_yO_{3-\delta}$ ($x = 0.05$, $y = 0.05$–0.2) solid electrolytes with optimal, low Ti content were chosen for our tests, according to previous results concerning the influence of Ti dopant concentration on chemical stability [16]. In this work the emphasis was given to the determination of influence of Y dopant concentration on the electrical and transport properties of these materials. The DC total electrical conductivity and proton, oxygen and electronic defects transference numbers determined from open cell voltage (OCV) measurements of electrochemical cells were presented and correlated with structural properties.

2. Experimental

2.1. Materials preparation

$Ba(Ce_{1-x}Ti_x)_{1-y}Y_yO_{3-\delta}$ ($x = 0.05$, $y = 0.05$–0.2) solid electrolytes were prepared by solid-state reaction method. Selected yttrium concentration range was typical for such dopants, limited by its solubility. Barium carbonate $BaCO_3$ (99.9%), cerium (IV) oxide CeO_2 (99.9%), TiO_2 nanopowder (99.7%) and $Y(NO_3)_3 \cdot 6H_2O$ (99.8%), all reagents as supplied by Aldrich Chemical Company, Inc. were used as starting materials.

The reactions of barium cerium–titanium oxide doped with yttrium can be written as follows (formation of NO_2 is assumed):

$$BaCO_3 + x(1-y)TiO_2 + (1-x)(1-y)CeO_2 + yY(NO_3)_3 \rightarrow$$

$$Ba(Ce_{1-x}Ti_x)_{1-y}Y_yO_3 + CO_2 + 3yNO_2 + \frac{y}{2}O_2 \qquad (3)$$

Appropriate amounts of starting powders were mixed and then impregnated with the correct amount of $Y(NO_3)_3$ water solution, then dried at 80 °C and finally calcined at 1200 °C for 24 h. The calcination conditions were determined basing on DTA-TG-MS and XRD results, as published previously [14–16]. The obtained materials were crushed in agate mortar, milled in the absolute alcohol suspension using planetary-rotational mill ("Pulverizette 6", Fritsh) and ZrO_2 grinding media ($\phi = 5$ mm, Tosoh), then formed in a pellet-die ($\phi = 25$ mm) at 25 MPa and isostatically pressed at 250 MPa. The bodies were sintered in air at 1600 °C for 24 h, then cut and polished using diamond tools to the required size and shape. Prepared samples were stored in the dessicator to avoid any secondary reactions with CO_2 and water vapor.

2.2. Determination of DC-conductivity and transference numbers

Prior to the electrical measurements the Pt electrodes ($\phi = 5$ mm) were screen-printed (Heraeus LP11 Pt paste) on both sides of the cut pellets ($\phi = 8$ mm, $d = 1.8$ mm) and fired at 850 °C for 5 min. Pellets with electrodes for determination of DC conductivity and transference numbers were mounted on the alumina tube using Ceramabond 569 ceramic adhesive to form the electrochemical cells, given by the general formula:

$$Pt, p(X_2)^{(1)}, p(H_2O)^{(1)} | Ba(Ce_{0.95}Ti_{0.05})_{1-y}Y_yO_{3-\delta} | p(X_2)^{(2)},$$

$$p(H_2O)^{(2)}, Pt \qquad (4)$$
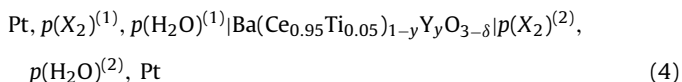
where $p(X_2)^{(1)}$ and $p(X_2)^{(2)}$ describe the hydrogen or oxygen atmospheres with defined pressures at both sides of the cells, while $p(H_2O)^{(1)}$ and $p(H_2O)^{(2)}$ are the water vapor pressures. The required gas compositions were obtained by mixing the gases (gas mixtures containing 5% H_2 in Ar or containing 21% O_2 in N_2) at a proper ratio, using the MKS gas flow controllers and passing them through a water bubblers at fixed temperature. Prior to each measurement, each sample was equilibrated at least 4–5 h under steady conditions. OCV of cells was measured as a function of temperature (500–800 °C) and the gas atmosphere gradients. The total DC

conductivity was measured at each temperature for non-gradient conditions. The transference numbers for oxygen ions (t_O), protonic defects (t_H) and electrons or holes (t_{el}) were determined according to the considerations and details given in [14], using the following formulas: in the case of oxygen rich atmospheres (21% O_2 in N_2 gas mixture and Ar were mixed at different ratios):

$$OCV = \frac{RT}{4F}(t_O + t_H) \ln \frac{pO_2^{(2)}}{pO_2^{(1)}} - \frac{RT}{2F} t_H \ln \frac{pH_2O^{(2)}}{pH_2O^{(1)}} \qquad (5)$$

in the case of hydrogen rich atmospheres (5% H_2 in Ar gas mixture and Ar were mixed at different ratios):

$$OCV = \frac{RT}{2F} \left(t_O \ln \frac{pH_2O^{(2)}}{pH_2O^{(1)}} - (t_O + t_H) \ln \frac{pH_2^{(2)}}{pH_2^{(1)}} \right) \qquad (6)$$

where OCV is the open cell voltage, t_O, t_H, are the transference numbers for oxygen ions and protonic defects, respectively, $pH_2O^{(1)}$, $pH_2O^{(2)}$, $pO_2^{(1)}$, $pO_2^{(2)}$, $pH_2^{(1)}$, $pH_2^{(2)}$ are water vapor, oxygen and hydrogen partial pressures at both sides: (1) and (2) of the cell, R is the universal gas constant, F is the Faraday constant, T is the absolute temperature.

For each type of gas atmosphere (rich in oxygen or rich in hydrogen), the OCV measurements were taken without the $p(H_2O)$ gradient and then without $p(O_2)$ (Eq. (5)) or $p(H_2)$ (Eq. (6)) gradients. The analysis of Eqs. (5) and (6) indicate that such approach allowed determining separately the transference numbers for oxygen ions and protonic defects. Namely, the total ionic transference number $t_{ion} = t_O + t_H$ was determined for $p(H_2O)^{(1)} = p(H_2O)^{(2)}$ for each type of atmosphere separately. Then, in the case of oxygen rich atmosphere the transference numbers for protonic defects were found for $p(O_2)^{(1)} = p(O_2)^{(2)}$ (Eq. (5)) and in the case of hydrogen rich atmosphere the transference numbers for oxygen ions were found for $p(H_2)^{(1)} = p(H_2)^{(2)}$ (Eq. (6)).

For both types of atmospheres the electronic transference numbers were calculated using the formula:

$$t_{el} = 1 - (t_O + t_H) \qquad (7)$$

where t_{el} is the transference number for electronic defects (electrons or holes).

3. Results and discussion

3.1. Crystallographic structure

XRD measurements were done using CuK_α radiation (Philips X'Pert) within the 2θ range 10–90° with the scan rate of 0.008° s^{-1}. Fig. 1 shows the comparison of obtained XRD spectra for different compositions. Previously, it was found that undoped material crystallize in orthorhombic Pmcn structure, while introduction of Ti leads to the ordering of the structure [14]. In the case of Y-doped samples (for Ti concentration $x = 0.05$) only slight differences in obtained spectra may be detected, as shown in the inset. The reflex positions are almost not affected by doping but the change of intensity ratio may be observed. Y^{3+} ion (0.090 nm) seems to be the ideal dopant for $BaCeO_3$ because the ionic radius is almost the same as Ce^{4+} (0.087 nm) [17].

Based on the measured XRD data and Rietveld method [18] the unit cell parameters and unit cell volumes were calculated, as shown in Fig. 2.

As can be seen the slight increase of a and c parameters with increasing concentration of Y can be observed. In the case of b parameter for the highest yttrium concentration ($y = 0.2$) the decrease comparing to samples with $y = 0.05$ and 0.1 was detected. It suggests that in the case of sample with nominal composition $Ba(Ce_{0.9}Ti_{0.05})_{0.8}Y_{0.2}O_{3-\delta}$ not all of the yttrium dopant incorporate
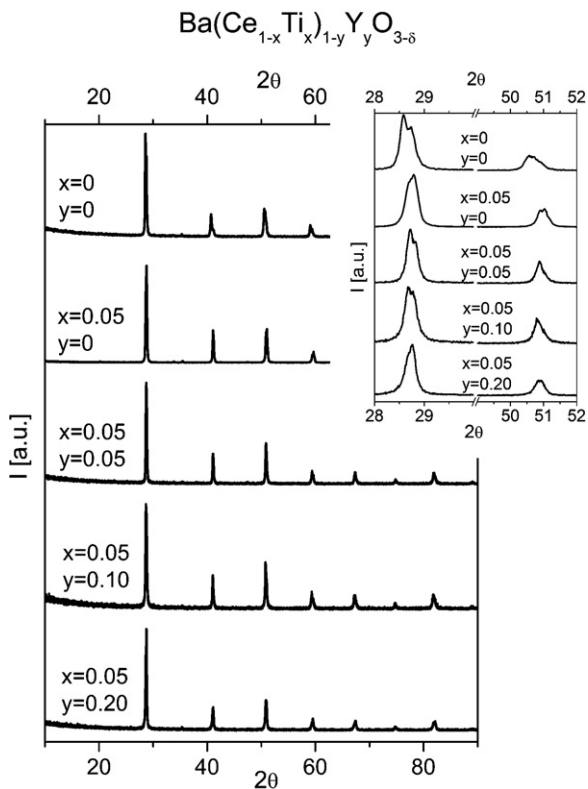
Fig. 1. XRD data of $Ba(Ce_{1-x}Ti_x)_{1-y}Y_yO_{3-\delta}$ ($x = 0$ and 0.05, $y = 0.00$–0.2) materials.

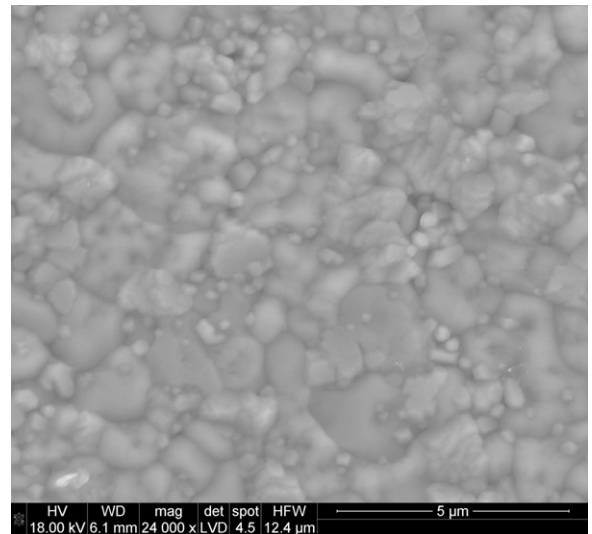**Fig. 3.** SEM micrograph of the $Ba(Ce_{0.95}Ti_{0.05})_{0.8}Y_{0.2}O_3$ fracture.

in the position of Ce(Ti) but may occupy different positions or segregate at grain boundaries. Additionally, it is worth to mention that simultaneous doping with Ti and Y allowed to extend typically reported solubility limit of Y dopant in $BaCeO_3$ lattice up to 20%.

3.2. Microstructure

The scanning electron microscope (SEM) observations were done using NOVA NANO SEM scanning electron microscope. Fig. 3
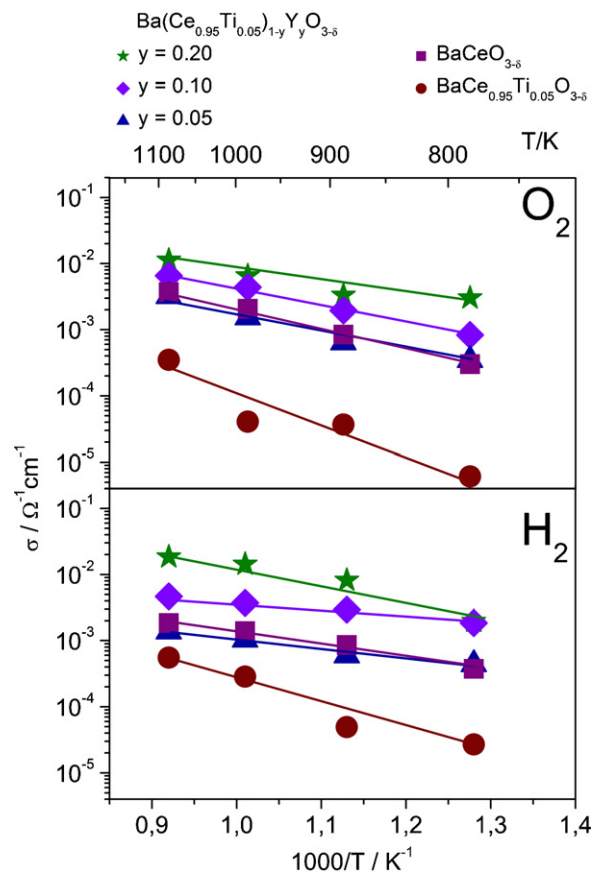

Fig. 2. Cell parameters and unit cell volume of $Ba(Ce_{1-x}Ti_x)_{1-y}Y_yO_{3-\delta}$ ($x = 0.05$, $y = 0.00$–0.2) materials as a function of composition.

Fig. 4. DC total conductivities measured as a function of temperature for undoped $BaCeO_{3-\delta}$, Ti doped ($BaCe_{0.95}Ti_{0.05}O_{3-\delta}$) and Y doped $Ba(Ce_{0.95}Ti_{0.05})_{1-y}Y_yO_{3-\delta}$ ($y = 0.05$, 0.1 and 0.2) samples at both O_2 and H_2-rich atmospheres.
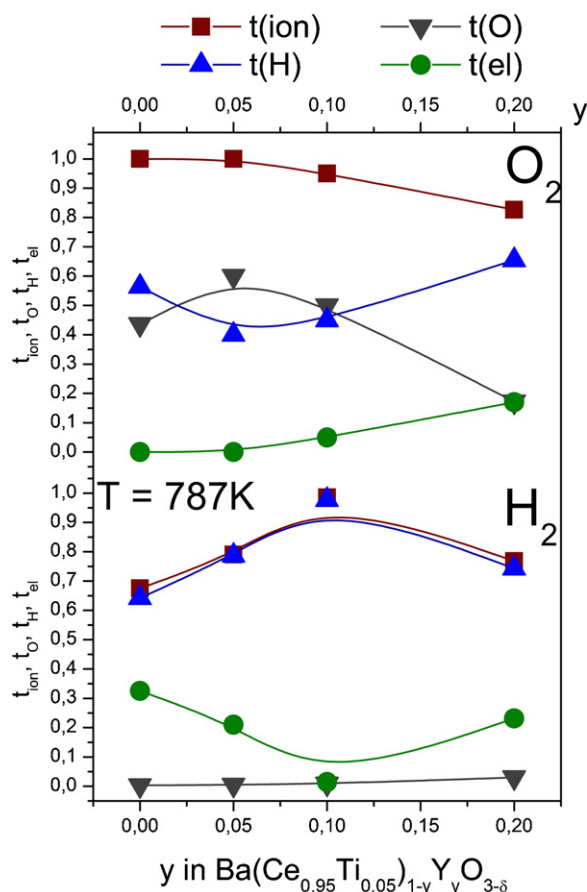
Fig. 5. Transference numbers plotted at $T = 787$ K, shown as a function of Y content, determined for O_2 and H_2-rich atmospheres.

Fig. 6. Transference numbers for $Ba(Ce_{0.95}Ti_{0.05})_{1-y}Y_yO_{3-\delta}$ sample, shown as a function temperature, determined for O_2 and H_2-rich atmospheres.

shows the example SEM image of the fractured surface of sintered $Ba(Ce_{0.9}Ti_{0.05})_{0.8}Y_{0.2}O_{3-\delta}$ sample. As can be observed the dense bulk materials with average grain size of several micrometers were obtained. Similar microstructure was observed in the case of all samples.

3.3. Electrical properties: DC conductivity and transference numbers

Fig. 4 shows the comparison for DC total conductivities measured as a function of temperature for undoped $BaCeO_{3-\delta}$, Ti doped ($BaCe_{0.95}Ti_{0.05}O_{3-\delta}$) and Y doped $Ba(Ce_{0.95}Ti_{0.05})_{1-y}Y_yO_{3-\delta}$ ($y = 0.05$, 0.1 and 0.2) samples at both O_2 and H_2-rich atmospheres. As can be seen, the doping by Ti causes the decrease of total conductivity compared to undoped material, accompanied by the modification of transport properties, as reported earlier [14]. Introduction of yttrium into the $Ba(Ce_{0.95}Ti_{0.05})_{1-y}Y_yO_{3-\delta}$ lattice leads to the opposite effect, the higher yttrium concentration, the higher total electrical conductivity was observed, for both gas atmospheres (H_2 and O_2-rich).

Figs. 5 and 6 show the representative results of transference numbers of ions ($t_{ion} = t_O + t_H$), protonic defects (t_H), oxygen (t_O) and electronic carriers (t_{el}), as determined from OCV measurements. Studied materials exhibit mixed ionic–electronic conductivity, where contribution of each type of electrical carrier (defect) is sample composition, temperature and gas atmosphere dependent. As shown in Fig. 5, plotted for $T = 787$ K, the highest values of protonic transference number can be observed in the case of $Ba(Ce_{0.95}Ti_{0.05})_{0.9}Y_{0.1}O_{3-\delta}$ sample ($y = 0.10$) for measurements taken at H_2-rich atmosphere (t_H close to 1). Observed dependence
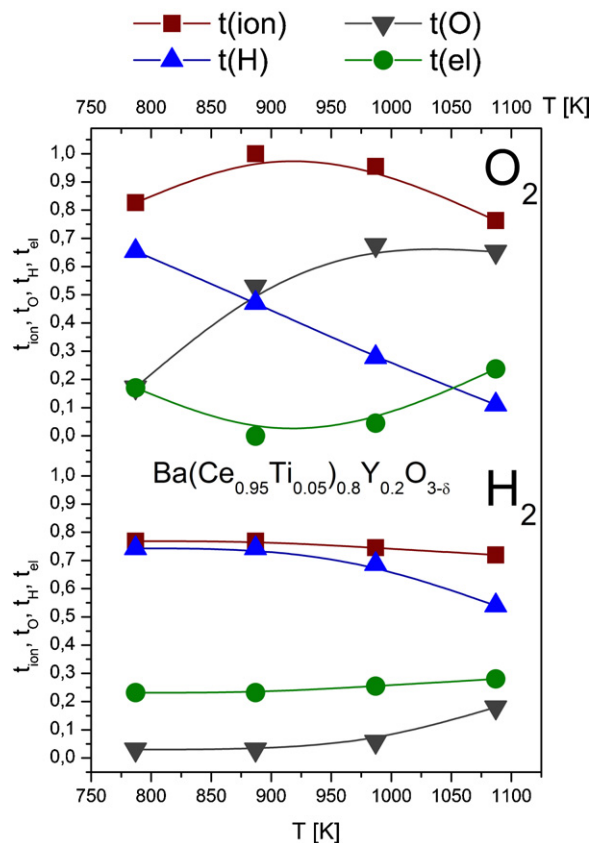
of transference numbers, t_O, t_H and t_{el}, on the composition, y (Fig. 6) may be generally correlated with the crystallographic data. In the case of $Ba(Ce_{0.95}Ti_{0.05})_{0.9}Y_{0.1}O_{3-\delta}$ sample ($y = 0.10$) the extreme values (maximum or minimum) of transference numbers corresponds well to the maximum of a lattice parameter and unit cell volume, V, as shown in Fig. 3. It is in agreement with results presented in [19] where similar correlation was found for $BaCeO_3$ modified with different dopants. In that work the highest ionic conductivity was observed when the doped composition has the largest cell volume.

The overall level of the protonic conductivity depends not only on proton transference number but also on total electrical conductivity, according to the dependence: $\sigma_H = t_H \cdot \sigma_{total}$. In this work the highest total and proton conductivities were observed in the case of $Ba(Ce_{0.95}Ti_{0.05})_{0.8}Y_{0.2}O_{3-\delta}$ sample ($y = 0.20$). Fig. 6 shows the dependence of transference numbers for this composition as the function of temperature. The higher temperature, the lower proton transference number and higher electronic transference numbers were observed, especially in the case of O_2-rich atmospheres. Taking into account relatively high protonic transference number ($t_H = 0.5$–0.7) and highest total electrical conductivity ($\approx 3 \times 10^{-2} \Omega^{-1} cm^{-1}$ at $T = 1073$ K) the $Ba(Ce_{0.95}Ti_{0.05})_{0.8}Y_{0.2}O_{3-\delta}$ ($y = 0.2$) material demonstrates the best electrical properties in the $Ba(Ce_{0.95}Ti_{0.05})_{1-y}Y_yO_{3-\delta}$ ($y = 0.05$, 0.1 and 0.2) series investigated in this work.

Further results of detailed crystallographic studies of $Ba(Ce_{0.95}Ti_{0.05})_{1-y}Y_yO_{3-\delta}$ materials would be vital to correlate the structure with enhancement of electrical properties in order to make available subsequent progress towards materials with higher protonic conductivity. Such XRD studies are under the way, the results will be published later.

4. Conclusions

Structural properties, total electrical conductivity and transference numbers of $Ba(Ce_{0.95}Ti_{0.05})_{1-y}Y_yO_{3-\delta}$ ($y = 0.05$, 0.1 and 0.2) materials were investigated. The results of XRD, SEM, DC electrical conductivity and OCV of electrochemical cells measurements presented in this paper indicate that the incorporation of titanium and yttrium into the $BaCeO_3$ lattice leads to the far modification of the crystallographic structure, electrical properties and charge transport mechanism. As reported previously, the incorporation of titanium into the $BaCeO_3$ lattice had the positive effect on chemical stability of material in the presence CO_2. From the other hand, the Ti-doping led to the decrease of total and ionic electrical conductivity of material, which was not preferred.

The subsequent introduction of yttrium to the $BaCeO_3$ lattice modified by Ti had the positive effect on electrical properties. The total electrical conductivity increased, the higher yttrium content the higher total conductivities were observed, independently on temperature and gas atmosphere composition. Also, the transference numbers were found to be strongly dependent on the composition. In general, doping with yttrium led to the increase of ionic transference numbers, comparing to the $BaCe_{0.95}Ti_{0.05}O_{3-\delta}$ material. It was found that the changes of protonic and ionic transference numbers with yttrium content may be correlated with the changes of lattice constant, a, and unit cell volume, V, determined from XRD measurements. The highest protonic transference numbers were found in the case of sample where the highest unit cell volume for $y = 0.10$, while the highest total and protonic conductivities were found in the case of sample for $y = 0.20$.

The analysis of currently published results concerning the influence of Y dopant on electrical properties of $Ba(Ce_{0.95}Ti_{0.05})_{1-y}Y_yO_{3-\delta}$ materials together with the previously published results concerning the materials' chemical stability in the presence of CO_2 allows to propose the $Ba(Ce_{0.95}Ti_{0.05})_{0.8}Y_{0.2}O_{3-\delta}$ as the best candidate for application in different electrochemical devices such as prototype fuel cells or pumps/membranes for hydrogen purification. The compromise on high chemical durability in the presence of CO_2 and relatively high total and ionic (protonic) conductivities of was reached for material with this composition ($x = 0.05$, $y = 0.20$).

References

[1] A. Kruth, G. Mather, J. Jurado, J. Irvine, Solid State Ionics 176 (2005) 703–712.
[2] H. Iwahara, T. Esaka, H. Uchida, N. Maeda, Solid State Ionics 3–4 (1981) 359–363.
[3] H. Iwahara, H. Uchida, K. Ono, K. Ogaki, J. Electrochem. Soc. 135 (1988) 529–533.
[4] I. Kosacki, H.L. Tuller, Solid State Ionics 80 (1995) 223–229.
[5] T. He, K.D. Kreuer, Yu.M. Baikov, J. Maier, Solid State Ionics 95 (1997) 301–308.
[6] A.S. Nowick, Y. Du, Solid State Ionics 77 (1995) 137–146.
[7] H. Iwahara, Solid State Ionics 86–88 (1996) 9–15.
[8] F.L. Chen, O.T. Sørensen, G.Y. Meng, D.K. Peng, J. Eur. Ceram. Soc. 18 (1998) 1389–1395.
[9] G. Ma, H. Matsumoto, H. Iwahara, Solid State Ionics 122 (1999) 237–247.
[10] M. Oishi, S. Akoshima, K. Yashiro, K. Sato, J. Mizusaki, T. Kawada, Solid State Ionics 179 (2008) 2240–2247.
[11] K.H. Ryu, S.M. Haile, Solid State Ionics 125 (1999) 355–367.
[12] S.M. Haile, G. Staneff, K.H. Ryu, J. Mater. Sci. 36 (2001) 1149–1160.
[13] K.D. Kreuer, Solid State Ionics 97 (1997) 1–15.
[14] P. Pasierb, E. Drożdż-Cieśla, M. Rekas, J. Power Sources 181 (2008) 17–23.
[15] P. Pasierb, Ann. Chim. Sci. Mater. 33 (Suppl. 1) (2008) 157–164.
[16] P. Pasierb, E. Drożdż-Cieśla, R. Gajerski, S. Łabuś, S. Komornicki, M. Rękas, J. Therm. Anal. Calorim. 96 (2) (2009) 475–480.
[17] R.D. Shannon, Acta Crystallogr. A32 (1976) 751–767.
[18] H.M. Rietveld, J. Appl. Crystallogr. 2 (1969) 65–71.
[19] J. Kikuchi, S. Koga, K. Kishi, M. Saito, J. Kuwano, Solid State Ionics 179 (2008) 1413–1416.